Hindawi
Mathematical Problems in Engineering
Volume 2021, Article ID 5430089, 16 pages
https://doi.org/10.1155/2021/5430089

Research Article

Grid Impact Assessment of Centralized and Decentralized Photovoltaic-Based Distribution Generation: A Case Study of Power Distribution Network with High Renewable Energy Penetration

Tamer Khatib and Lama Sabri

Department of Energy Engineering and Environment, An-Najah National University, Nablus, State of Palestine

Correspondence should be addressed to Tamer Khatib; t.khatib@najah.edu

Received 10 April 2021; Revised 3 June 2021; Accepted 28 June 2021; Published 7 July 2021

Academic Editor: Xiao-Shun Zhang

This paper presents a grid impact assessment of a 5 MWp photovoltaic-based distribution unit on a 33 kV/23 MVA power distribution network with high penetration of renewable energy generation. The adapted network has an average load demand of 23 MVA, with a 3 MWp centralized PV system, and a number of decentralized PV systems of a capacity of 2 MWp. A grid impact assessment is done to an additional 5 MWp of PV generation as a centralized system as well as a number of decentralized systems. Power flow analysis is conducted to the grid considering different generation loading scenarios in order to study grid performance including active and reactive power flow, voltage profiles, distribution power transformers loading, transmission lines ampacity levels, and active and reactive power losses. On the other hand, the distribution of the decentralized systems is done optimally considering power distribution transformer loading and available area using the geographical information system. Finally, an economic analysis is done for both cases. Results showed that grid performance is better considering decentralized PV systems, whereas the active power losses are reduced by 13.43% and the reactive power losses are reduced by 14.48%. Moreover, the voltage of buses improved as compared to the centralized system. However, the decentralized PV systems were found to affect the power quality negatively more than the centralized system. As for the economic analysis, the decentralized PV system option is found slightly less profitable than the centralized system, whereas the simple payback period is 9 and 7 years, respectively. However, decentralized PV systems are recommended considering the technical implications of the centralized PV system.

1. Introduction

The technology of distributed generation (DG) is defined as a small-scale generation unit that is installed at the consumer side. There are different types of DGs, whereas they could be from conventional resources such as diesel generators and combustion turbines or renewable energy resources such as solar, wind, and biomass energies [1].

The integration of photovoltaic distributed generation (PVDG) into a distribution system can be a beneficial solution as it is reliable, reduces peak load, reduces grid losses, and supports power quality [2]. Meanwhile, with high penetration levels, the impact of PVDG would be negative, such as reverse power flow, voltage fluctuations, and system instability [3]. Thus, power flow, power quality, and short-circuit analyses are very essential to assess the impact of PVDG on the grid before its installation.

The main characteristic of solar power is the intermittent nature and unreliable sources of generating power when connected to the grid, due to many reasons such as weather conditions (temperature and irradiance), diurnal variation, and mismatch. As a result, voltage fluctuation can happen and cause problems and consequently reduce voltage quality [4, 5].

Besides that, when PV output power changes rapidly, the area control error of two or more interconnected areas may exceed its prescribed limit. Finally, large uncontrolled PV penetration may change the dispatch of regulating units in the utility causing a violation in dispatch regulating margins [6].

Due to these negative impacts, standards have been imposed to control these impacts, such as IEEE 1547 that provides standards of voltage fluctuation range when interconnection between utility electric power systems and distributed energy resources occurs. In addition to that, many researchers have investigated the impact of high penetration levels of renewable energy on the power grid. In [3], an unacceptable voltage rise is reported and analyzed with 50% of PV penetration, especially at noontime [3]. Meanwhile, according to [7], with high penetration levels of renewable energy, losses can be increased [7]. Similarly in [8], the reverse power problem is discussed, whereas it is claimed that when the out power does not match the demand, it is a serious challenge for the network since all power transformers and protection components are designed for unidirectional power flow [8]. This can make overloading of the distribution feeders and excessive power losses. Finally, in [9], the negative impact of high penetration of renewable energy on harmonics is discussed. Following that, many authors have discussed the methodology and the technical impact of grid impact studies. In [10], procedures of photovoltaic penetration impact on the grid are analyzed and studied. The authors proposed a model that considers the uncertainty of solar power generation and stochastic assessment methods that could accurately estimate the state of the operation of the network with different levels of penetration of solar photovoltaics. In [11], the authors estimate the impact of rapid PV output fluctuations on the power quality in an existing LV grid by performing load flow analyses.

Therefore, a grid impact study should be done on the power network before installing any renewable-energy-based distributed generation. Thus, this study proposes a framework of grid impact study for PVDG by analyzing the following: (i) the power flow analysis of the system is done before and after the installation of the distributed generation unit to evaluate the impact of PVDG on the power system. This process assesses voltage levels, system power flow, and system's power losses. This analysis should be done considering different operational scenarios considering generation and demand. (ii) The short-circuit analysis is done to check the contribution of the newly added renewable energy system to the network of any short circuit considering different voltage contributions to the fault location. (iii) The harmonics analysis of the system should be done to evaluate the impact of the newly added system on the power quality of the system. (iv) The paper discusses impact of centralized and decentralized PVDG in medium-scale distribution networks considering grid health conditions. The contribution of this paper is represented by the technical information and analysis provided for the network in Palestine in specific and distribution network in general with high penetration of renewable energy.

2. The Adapted Case Study

Palestinian territories suffer from the scarcity of conventional energy sources, high population growth, and rising prices of energy. Thus, this would lead Palestine to a developing energy crisis [12]. In 2018, Palestine's total energy demand reached around 5,800 GWh, in which Israel Electric Company (IEC) covered around 92.6% of this demand. The rest of the energy supplies are from Jordan (1.5%), Egypt (0.6%), and Gaza Power Plant (4.4%). Meanwhile, renewable energy sources accounting for 0.9% [13]. The high energy imports from the IEC had left the Palestinian Authority (PA) with an estimated debt of 574 million USD [13]. On the other hand, the cost of energy (CoE) is relatively high in Palestine, whereas CoE is approximately 0.19 USD/kWh for the residential sector. On the other hand, the CoE in Israel is approximately 0.14 USD/kWh [13]. It is expected that seasonal power shortages will be emerging in the West Bank following a demand growth of 3.5% per year until 2030.

On the other hand, Palestine has some potential for renewable energy sources that could make a change for the whole situation. For instance, Palestine has an estimated annual average daily solar energy in the range of 5.4 kWh/m^2–6 kWh/m^2 with sunshine hours over 3,000 hours per year. However, this average daily solar energy goes as low as 2.6 kWh/m^2 in December and reaches up to 8.4 kWh/m^2 in June [14–18]. Based on that, the PA, through the Palestinian Energy and Natural Resources Authority (PENRA), has set several policies for encouraging investment in PV systems. Moreover, Palestine Investment Promotion Fund (PIF), which is a public body connected to the PA, had set PV systems as Palestine's major investment opportunities for local and international investors, with an estimated market size of $50 million [19]. Following that, many projects have been implemented in Palestinian cities. In summary, there are 39 MW installed PV systems, while 93 MWp of PV systems are still under development. Moreover, there are about 24 MWp PV systems proposed officially for approval, with several MWp (s) of PV system in planning.

In Palestine, there is a governorate called Tubas. This governorate is powered by a 33 kV distribution network. The current penetration level of renewable energy in this network is 21.74%, which is somehow fine. However, recently, there is a new project of 5 MWp to be installed in the network, whereas a lot of disputes are around this project. The installation of this project will increase the penetration level to be 43.47%. This will put the network in a critical situation such as reverse power flow and high-power losses. Thus, it is aimed in this research to determine the impact of such a proposal on the network. Moreover, as such a proposal is assumed to be not suitable as a centralized system, an alternative solution is investigated that is the installation of a group of decentralized systems instead of one centralized system to mitigate the negative impact of the system on the grid.

2.1. Modeling of the Adapted Power Network. To produce precise data on network demand, voltage levels, and losses, data collection was conducted including a one-line diagram of Tubas LV and MV power network including loading profiles, transmission lines characteristics, power transformer characteristics, circuit breaker characteristics, current coupling points, sources of power, grid capacity, and present power factor (PF) levels at LV power transformers.

Tubas power grid is getting electricity supply by 161/33 kV substation called Tayaser power substation with a power capacity of 23 MVA. Other power substations are providing the power grid with power such as AlJalameh power point (8 MVA), Qabatiya power point (2 MVA), Alzawiya power point (5 MVA), and Nassaria power point (5 MVA). These MV connections are with the IEC (Israel Electricity Corporation) grid. There are some local PV power systems in the grid that are 2 MWp distributed systems and a 3 MWp centralized plant. The loads are mostly domestic, and few of them are commercial, agricultural, and industrial.

In this research, all power coupling points with IEC were considered as slack buses with an X/R value that is equal to 13.2154, while PV power systems were considered as distributed generation units.

The average load demand of the network is 23 MVA, based on daily records of consumption. An average daily load curve is demonstrated in Figure 1. These information are collected from the stakeholder by the authors of this paper. The daily load profile corresponds to a typical load profile for a distribution grid in the region with mostly domestic clients with peak demand at noon (16 MVA) and afternoon (20 MVA) with lower consumption during the night (14–12 MVA) and early morning (10 MVA).

From the load profile, it can be seen that during the solar day and specifically from 10:00 AM to 2:00 PM, the maximum power demanded is about 14–16 MVA, which means that the generating power of any distributed generation source should not exceed these values. Otherwise, reverse power will occur.

In this research, the model was developed based on a one-line diagram. In general, the MV grid is built mainly from overhead line (OHL) 33 kV voltage level and underground cables. The OHLs are usually FEAL-type conductors of 50, 95, and 120 mm^2. The UGCS is usually TSLE or DKBA type of 3×120 mm^2, 3×150 mm^2, or 3×240 mm^2. Most of them are made of copper and some are of aluminum material.

There is a total number of 78 buses at 33 kV, mostly power consumption nodes (57 nodes), including the concentrated consumption of Qabatiya, Anza, Zawiya, Zababeda, Wadi Douq, Um Al Toot, Tilfit, Tineen, Raba, Private project, Mghayer, Merkeh, Jarba, Jalqumous, Dream Land, Beer Al-Basha, AUU, Al Mtelleh, Wadi Al Faraa, Ras Al Faraa, Keshda, and Faraa Camp. The loads in Tubas, Aqqaba, Atoof, Kufeir, and Tammun were modeled in detail. The load from Qabatiya, Anza, Alzawiya, Zababeda, Wadi Douq, Um Al Toot, Tilfit, Tineen, Raba, Private project, Mghayer, Merkeh, Jarba, Jalqumous, Dream Land, Beer Al-Basha, AUU, and Al Mtelleh were modeled as total load (in node Qabatiya). The loads associated with Wadi Al Faraa, Ras Al Faraa, Keshda, and Faraa Camp were also modeled as cumulated loads.

Based on the information mentioned above, the power flow analysis of the network was performed using Newton–Raphson method in ETAP software.

3. Grid Impact Assessment Methodology

When planning for DG size and location, there is no specific rule for that. Some researchers use the role of thumps, while others use optimization techniques. Anyway, in simple words, there is a role of thump for calculating the suitable size of distributed generation assumes that a DG system that covers 30% of the energy consumed during the solar day subject to have a rated power that is lower than the minimum local peak point during the solar day is fine.

By looking at Figure 1, we can say that the local peak value is 14 MVA, the energy consumption during the solar day is about 130 MWh (PF is assumed 0.9). Meanwhile, the yield factor for PV systems in Palestine is about 4.8 kWh/kWp per day. Assume that we need to cover 30% of the load demand. The required size of a PV system is about 8 MWp. Meanwhile, with the proposed system, the capacity of the total PV system is 10 MWp. Thus, there is a dire need for careful grid impact assessment.

In this research, the conducted grid impact assessment has three main assessments that are load flow assessment, short-circuit assessment, and harmonics quality assessment.

3.1. Load Flow Analysis. In any power system, the power that is generated from the station is transmitted through transmission lines to the loads. The flow of active and reactive power is known as load flow or power flow. Load flow analysis is an important tool to determine the steady-state operation of a power system. Load flow analysis provides a systematic mathematical approach to determine the bus voltages, phase angles, active, and reactive power flow through different branches, generators, transformer settings, and load under steady-state conditions [20].

The information of load flow is essential for analyzing the effective alternate plan for the system expansion to meet the increasing load demand. The load flow analysis helps identify the over-/underloaded lines and transformers as well as over-/undervoltage buses in the system. It is used to study the optimum location of capacity and their size to improve the unacceptable voltage profile [21].

The resulting equations in terms of power, known as the power flow equations, become nonlinear and must be solved by iterative techniques using numerical methods [22], such as Newton–Raphson method. These equations can be written in the terms of either the bus admittance matrix (YBUS) or the bus impedance matrix. With the availability of fast digital computers, all kinds of power system studies, including load flow, can now be carried out conveniently.

3.1.1. Newton–Raphson Method. There are several methods of solving the nonlinear system of equations. The most efficient one is the Newton–Raphson Method. This method begins with initial guesses of all unknown variables such as voltage magnitude and angles at load buses and voltage angles at generator buses. Next, a Taylor series is written, for each of the power balance equations included in the system of equations. The result is a linear system of equations that can be expressed as follows:

$$\begin{bmatrix} \Delta\theta \\ |\Delta V| \end{bmatrix} = -J^{-1} \begin{bmatrix} \Delta P \\ \Delta Q \end{bmatrix},$$

$$\Delta P_i = -P_i + \sum_{k=1}^{n} |V|_i |V|_k \left(G_{ik} \cos \theta_{ik} + B_{ik} \sin \theta_{ik}\right), |V|_i |V|_k \left(G_{ik} \cos \theta_{ik} - B_{ik} \sin \theta_{ik}\right),$$

$$\Delta Q_i = -Q_i + \sum_{k=1}^{n} \tag{1}$$

$$J = \begin{bmatrix} \dfrac{\partial\Delta P}{\partial\theta} & \dfrac{\partial\Delta P}{\partial|V|} \\ \dfrac{\partial\Delta Q}{\partial\theta} & \dfrac{\partial\Delta Q}{\partial|V|} \end{bmatrix},$$

where ΔP and ΔQ are called the mismatch equations and J is a matrix of partial derivatives known as a Jacobian.

The linearized system of equations is solved to determine the next guess $(m+1)$ of voltage magnitude and angles based on

$$\theta^{m+1} = \theta^m + \Delta\theta,$$
$$|V|^{m+1} = |V|^m + \Delta|V|. \tag{2}$$

The process continues until a stopping condition is met. A common stopping condition is to terminate if the norm of the mismatch equations is below a specified tolerance. Outline of the solution of the power flow problem is as follows:

(1) Make an initial guess of all unknown voltage magnitudes and angles. It is common to use a "flat start" in which all voltage angles are set to zero and all voltage magnitudes are set to 1.0 p.u.
(2) Solve the power balance equations using the most recent voltage angle and magnitude values.
(3) Linearize the system around the most recent voltage angle and magnitude values.
(4) Solve for the change in voltage angle and magnitude.
(5) Update the voltage magnitude and angles.

Check the stopping conditions; if met, then terminate, or else go to step 2.

3.2. Short-Circuit Analysis. The key application of short-circuit calculations is in the design of the protection system. Short-circuit analysis is mainly needed to determine the three-phase fault level at one or more nodes (buses) in the system. The three-phase fault level is used to assess the short-circuit current interruption potential of the circuit breakers [23].

A general representation of a balanced three-phase fault is shown in Figure 2, where F is the fault point with impedances Z_f and Z_g. Figure 3 shows the sequences networks interconnection diagram [24].

From Figure 3, it can be noticed that the only one that has an internal voltage source is the positive-sequence network. Therefore, the corresponding currents for each of the sequences can be expressed as follows:

$$I_{a0} = 0,$$
$$I_{a2} = 0, \tag{3}$$
$$I_{a1} = \frac{1.0\angle 0^\circ}{Z_1 + Z_f}.$$

If the fault impedance Z_f is zero,

$$I_{a1} = \frac{1.0\angle 0^\circ}{Z_1}. \tag{4}$$

Equation (4) is substituted into the following equation:

$$\begin{bmatrix} I_{af} \\ I_{bf} \\ I_{cf} \end{bmatrix} = \begin{bmatrix} 1 & 1 & 1 \\ 1 & a^2 & a \\ 1 & a & a^2 \end{bmatrix} \begin{bmatrix} 0 \\ I_{a1} \\ 0 \end{bmatrix}. \tag{5}$$

Solving the above equation,

$$I_{af} = I_{a1} = \frac{1.0\angle 0^\circ}{Z_1 + Z_f},$$
$$I_{bf} = a^2 I_{a1} = \frac{1.0\angle 240^\circ}{Z_1 + Z_f}, \tag{6}$$
$$I_{cf} = a I_{a1} = \frac{1.0\angle 120^\circ}{Z_1 + Z_f}.$$

Since the sequence networks are short-circuited over their own fault impedance,

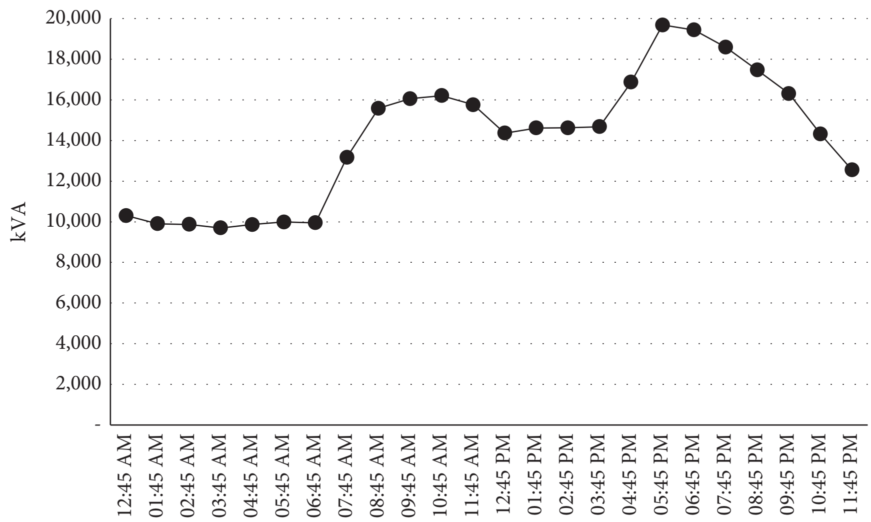

Figure 1: Characteristic daily load curve for the network.

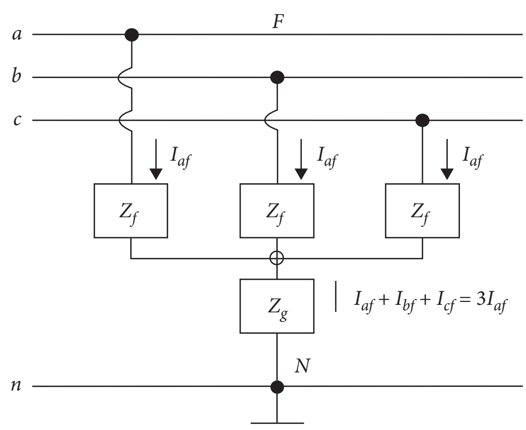

Figure 2: General representation of a balanced three-phase fault [20].

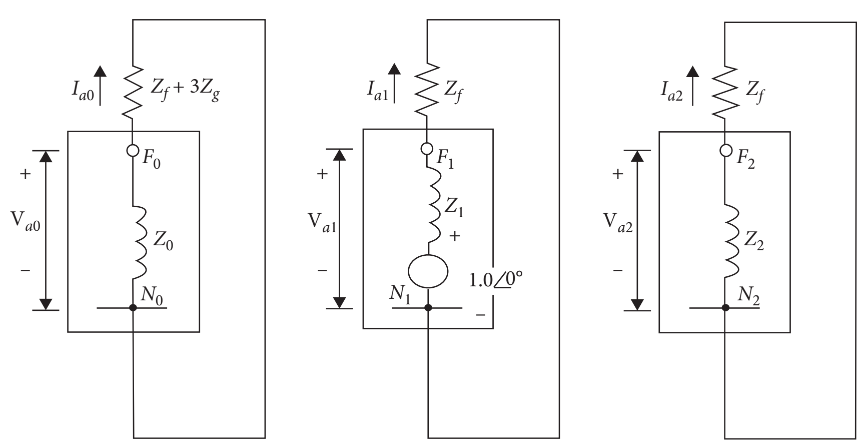

Figure 3: Sequence network diagram of a balanced three-phase fault [24].

$$V_{a0} = 0, \tag{7}$$

$$V_{a1} = Z_f I_{a1}, \tag{8}$$

$$V_{a2} = 0. \tag{9}$$

Equations (7)–(9) are substituted into the following equation:

$$\begin{bmatrix} V_{af} \\ V_{bf} \\ V_{cf} \end{bmatrix} = \begin{bmatrix} 1 & 1 & 1 \\ 1 & a^2 & a \\ 1 & a & a^2 \end{bmatrix} \begin{bmatrix} 0 \\ V_{a1} \\ 0 \end{bmatrix}. \tag{10}$$

Therefore,

$$\begin{aligned} V_{af} &= V_{a1} = Z_f I_{a1}, \\ V_{bf} &= a^2 V_{a1} = Z_f I_{a1} \angle 240^\circ, \\ V_{cf} &= a V_{a1} = Z_f I_{a1} \angle 120^\circ. \end{aligned} \tag{11}$$

The line-to-line voltages are

$$\begin{aligned} V_{ab} &= V_{af} - V_{bf} = V_{a1}\left(1 - a^2\right) = \sqrt{3}\, Z_f\, I_{a1} \angle 30^\circ, \\ V_{bc} &= V_{bf} - V_{cf} = V_{a1}\left(a^2 - a\right) = \sqrt{3}\, Z_f\, I_{a1} \angle - 90^\circ, \\ V_{ca} &= V_{cf} - V_{af} = V_{a1}\,(a - 1) = \sqrt{3}\, Z_f\, I_{a1} \angle 150^\circ. \end{aligned} \tag{12}$$

If Z_f is equal to zero,

$$\begin{aligned} I_{af} &= \frac{1.0\angle 0^\circ}{Z_1}, \\ I_{bf} &= \frac{1.0\angle 240^\circ}{Z_1}, \\ I_{cf} &= \frac{1.0\angle 120^\circ}{Z_1}. \end{aligned} \tag{13}$$

The phrase voltages become

$$V_{af}, V_{bf}, V_{cf} = 0. \tag{14}$$

The line voltages become

$$V_{a0}, V_{a1}, V_{a2} = 0. \tag{15}$$

3.3. Power Quality Assessment. The aim of the harmonic analysis is to determine the distribution of harmonic currents, voltages, and harmonic distortion indices in a power system. This analysis is then extended to the study of resonant conditions and harmonic filter designs and also other effects of harmonics on the power system, that is, notching and ringing, neutral currents, saturation of transformers, and overloading of system components [25].

For the first step, a frequency scan is obtained, which plots the variation of the impedance modulus and the phase angle of the selected bus with frequency variation or generates *R–X* impedance plots. This allows the determination of the resonant frequencies. Harmonic current flows in the lines are measured, and the network, which is presumed to be linear at each stage of the calculations with the added constraints, is solved to obtain harmonic voltages [25]. The equations shall contain the harmonic distortion indices.

4. Economic Evaluation Criteria

Different indicators were considered in order to compare centralized system and decentralized system for economic analysis as follows; the simple payback period (SPP), the net present value (NPV), and internal rate return (IRR) that are significant economic parameters will be used to evaluate the feasibility for investors to invest into a rooftop PV system.

The simple payback period of investments is defined as the ratio of the initial investment's size to the value of the estimated cash flow as follows:

$$\text{SPP} = \frac{IC_0}{CF_1}, \tag{16}$$

where IC_0 is the value of the invested capital and CF_1 is the cash flow. This value is achieved as the result of the implementation of energy-saving measures and savings in operating costs or expected to be achieved at the stage of project development after the end of the calendar year.

Net present value (NPV) is also used in this research. NPV is a method that is used to determine the current value of all future cash flows generated by a project, including the initial capital investment. The formula of NPV is as follows:

$$\text{NPV} = \frac{CF}{(1+i)^n} - \text{initial investment}, \tag{17}$$

where n is the investment period and i is the discount rate of return that could be earned in alternative investment.

Finally, the discount rate (IRR) is used as well. IRR is the discount rate that makes the NPV of a project zero. In other words, it is the expected compound annual rate of return that will be earned on a project or investment.

The formula for IRR is as follows:

$$0 = NPV = \sum_{n=0}^{N} \frac{CF_n}{(1+\text{IRR})^n}, \tag{18}$$

where N is the holding period.

5. Results and Discussion

5.1. Results for Power Flow Analysis of the Adapted Power Distribution Network. In general, the voltages of the 33 kV distribution points of the Tubas network are facing many under voltages. Figure 4 shows the thermal contouring map of the network.

As indicated in Figure 4, the warmer color indicates lower voltage levels, while the green color means a normal situation. The network situation is critical. In general, renewable energy penetration is about 21.74%, which is very high for such types of networks under similar conditions.

The results of power flow revealed that ten transformers were overloaded as demonstrated in Table 1. Also, an enormous

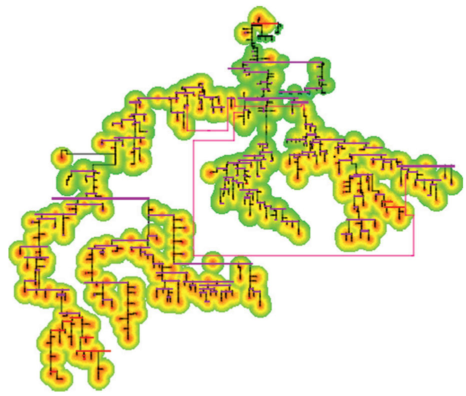

Figure 4: Power flow analysis of Tubas power distribution grid.

Table 1: Loading levels, conditions, and PV connected to the transformers.

Transformers	Condition	Rating/limit	Unit	Operating	% operating	PV connected
Afaq, Dreamland	Overload	0.400	MVA	0.61	153.6	0
Aqqaba water treatment	Overload	0.100	MVA	0.13	131.3	0
Ashraf Khader	Overload	0.160	MVA	0.27	167.8	0
Hawooz Aqqaba	Overload	0.250	MVA	2.4	959	97 kW
Maslamani F.C.	Overload	0.400	MVA	0.47	116.6	500 kW
Meselya Water East Stn	Overload	0.630	MVA	0.76	120.5	0
Qetaf Co	Overload	0.160	MVA	0.52	326.8	0
School Taysaer	Overload	0.160	MVA	0.2	122.8	0
Tubas Park	Overload	0.100	MVA	0.1	103.7	0
Zoghioul, ZA	Overload	0.160	MVA	0.44	272	15 kW

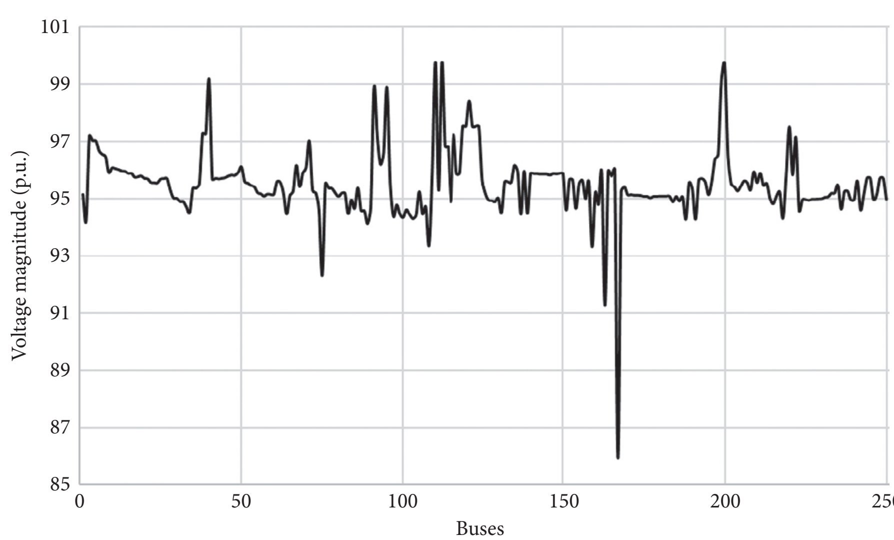

Figure 5: Voltage profile of Tubas network.

number of buses were undervoltage. Moreover, there were a lot of buses and PV arrays that are in marginal condition considering voltage level as can be seen in Figure 5.

The total losses in the network are 7.03% of the fully active power generation, while the reactive power losses are 14.34% of the fully reactive power generation.

5.2. Results for Centralized and Decentralized PVDG System Impact on the Grid. In this section, two scenarios are studies: first, installing the proposed 5 MWp system as a centralized system at the proposed location by the operator at 33 kV level and, second, proposing a group of small-scale PV systems to be at the 0.4 kV network.

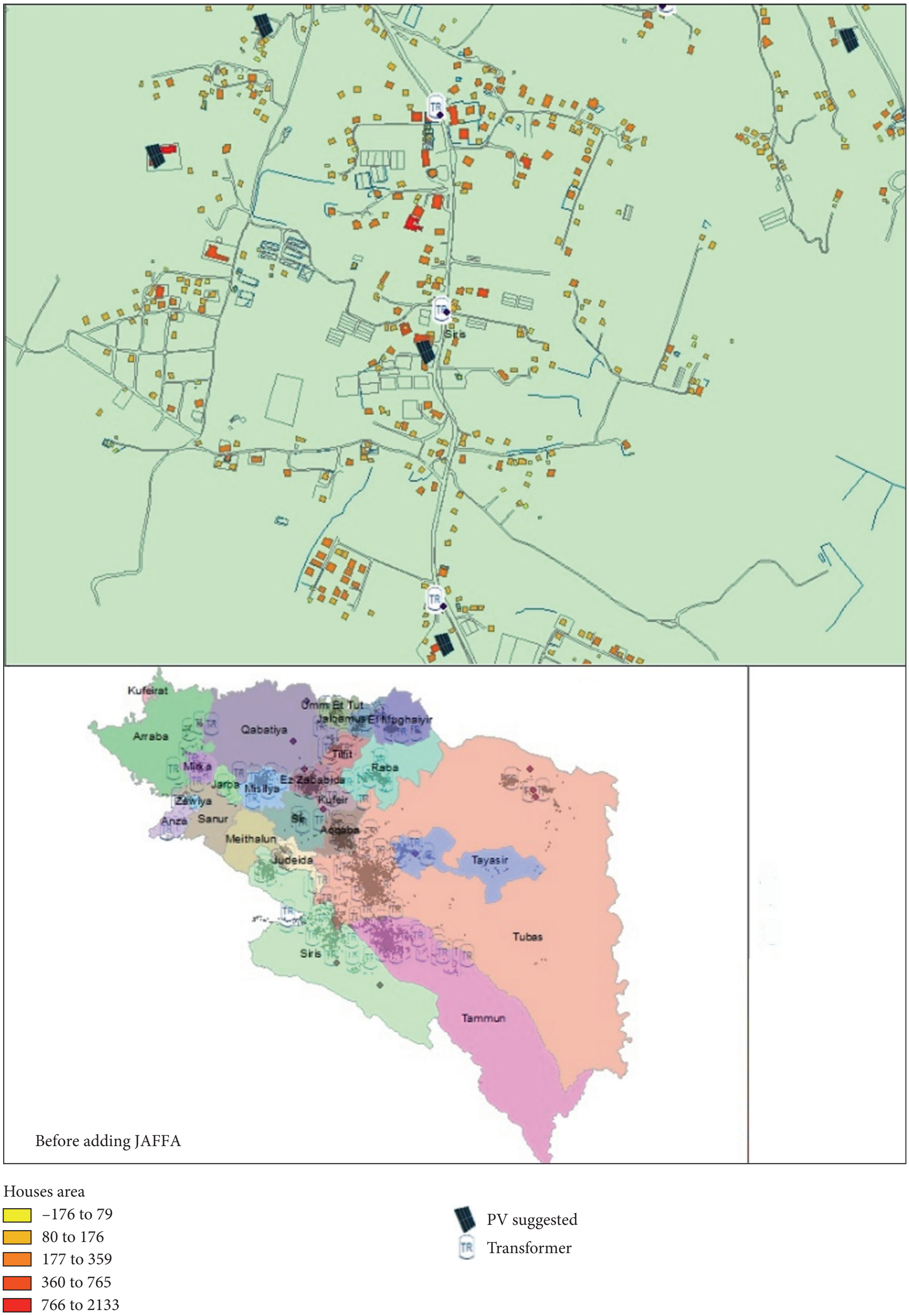

Figure 6: Tubas with suggested PVDG on rooftops.

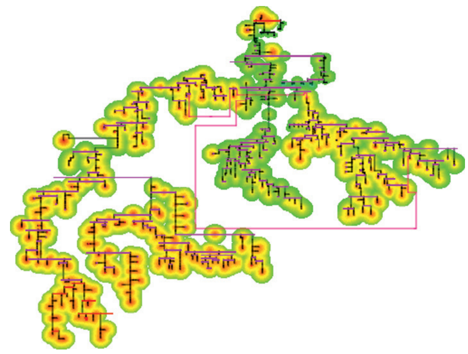

Figure 7: Thermal contouring map for the centralized case.

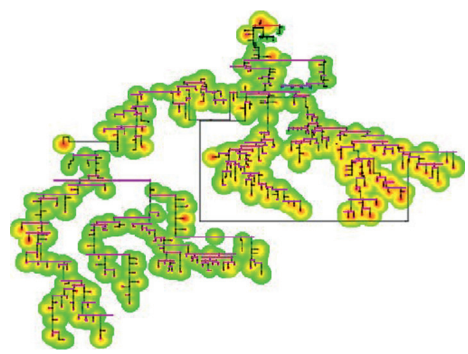

Figure 8: Thermal contouring map for the decentralized case.

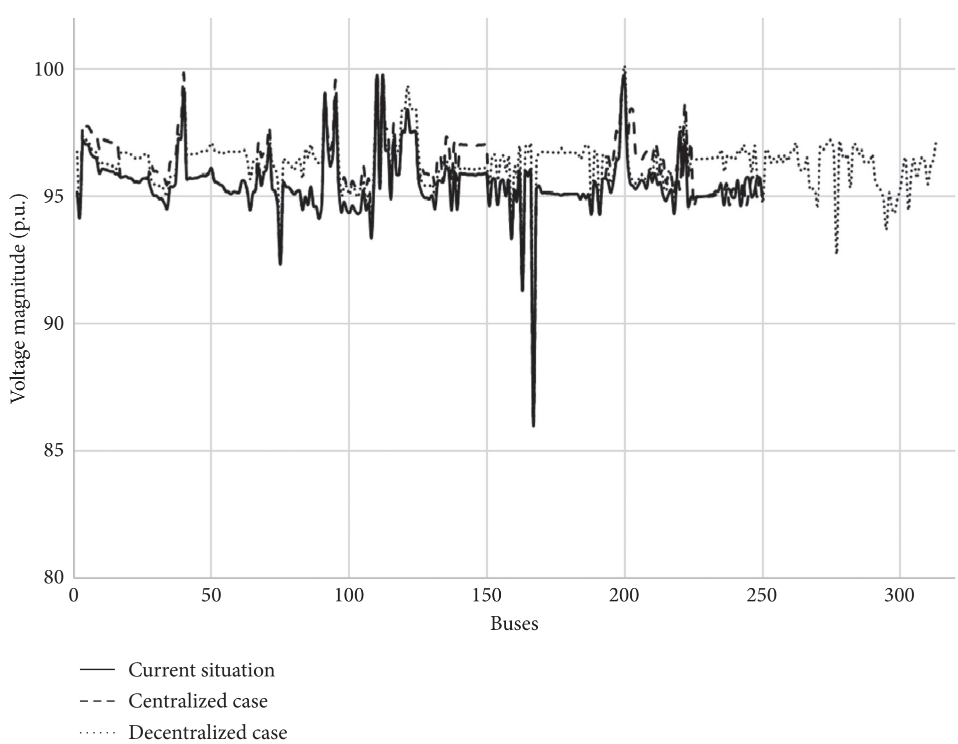

Figure 9: Voltage profile of Tubas network in the three cases.

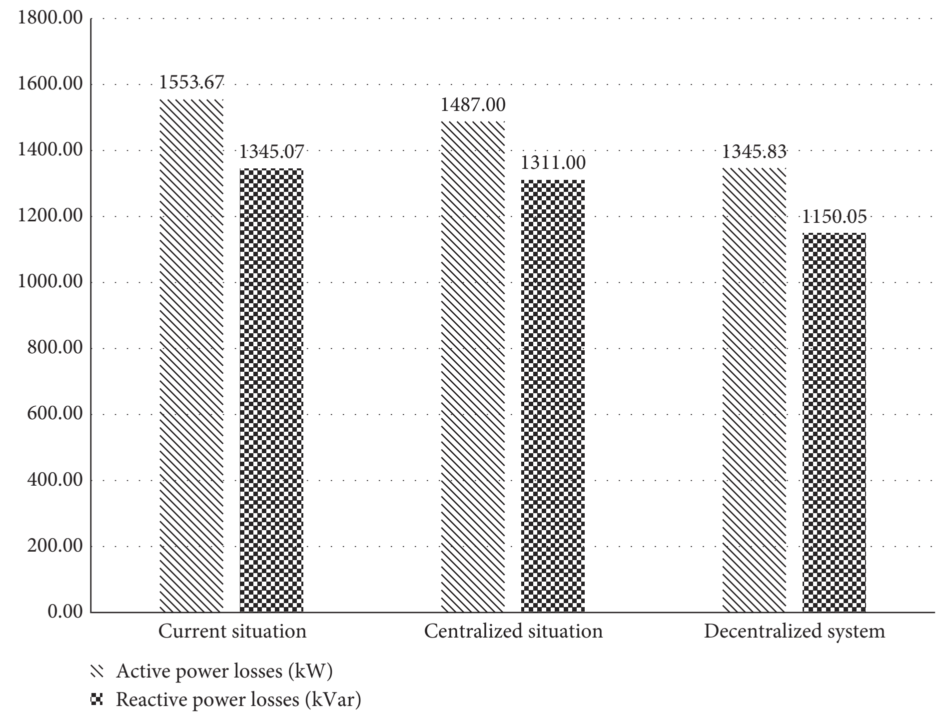

Figure 10: Active and reactive power losses.

Table 2: Point of common coupling loading.

	P (MW)	Q (MVar)	S (MVA)	% PF	% loading
Current situation	8.57	2.90	9.05	94.72	39.34
Centralized	4.19	2.91	5.10	82.13	22.15
Decentralized	7.73	2.81	8.23	93.98	35.77

Table 3: Description of Tubas network in the three cases.

Critical situation	Current situation	Centralized case	Decentralized case
Undervoltage buses	176	124	36
Overvoltage buses	0	0	0
Overloaded transformers	10	12	11

Table 4: Highest short-circuit current in the three cases.

	Highest short-circuit current (kA)	% increase in short-circuit current
Current situation	64.85	—
Centralized case	67.51	4.11
Decentralized case	68.93	6.30

To implement the decentralized approach of the system, the results obtained from power flow are used to have the voltage of transforms as well as its capacity. After that, it is suggested to install PVDG on these transformers by considering 25% of transformer capacity. Here, any other PV system installed previously is considered within the 25% assumption. Available areas around each transformer are also considered. Here, all the small PV systems are considered rooftop PV systems. However, the area of the suggested PVDG was not enough to mount 5 MWp in the actual houses, so it was reduced to 4.2348 MWp to be compatible with the real situation.

Here, another power flow is performed after installing the decentralized system on the overloaded transformers as

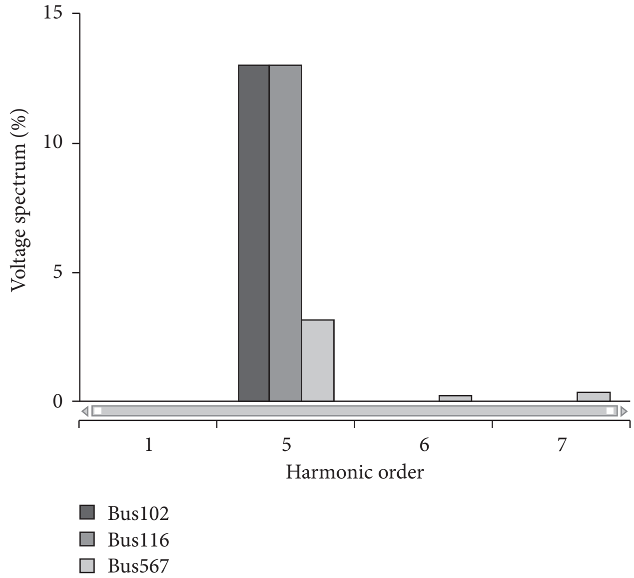

(a)

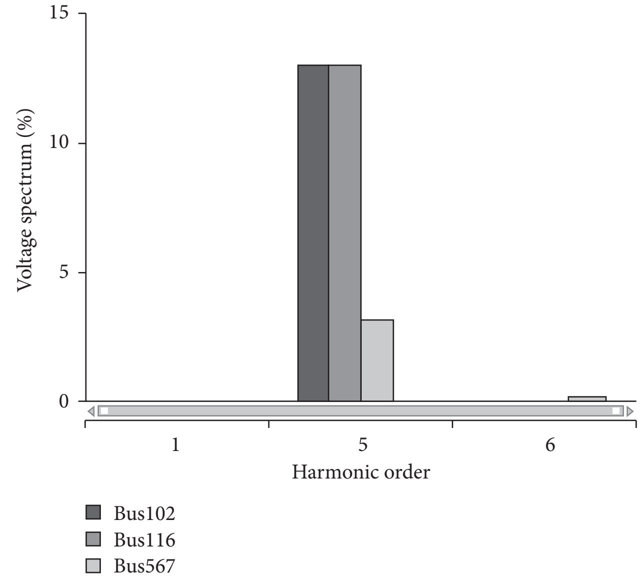

(b)

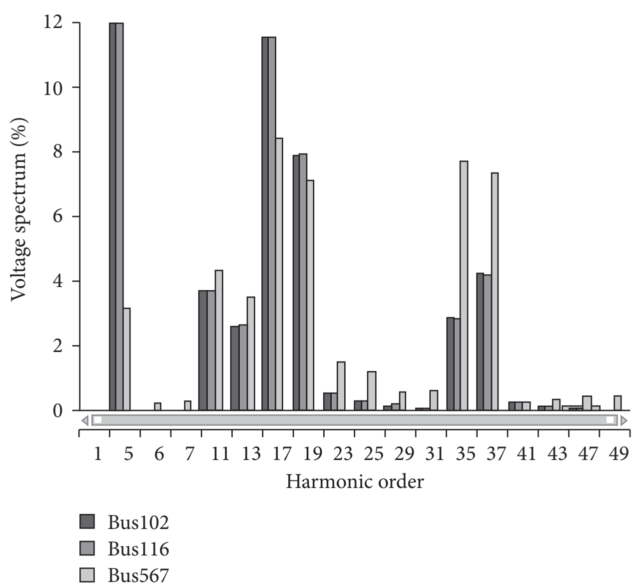

(c)

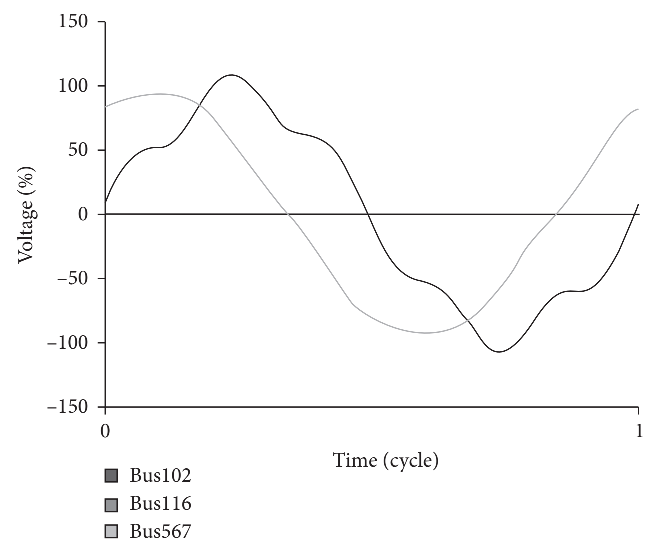

(d)

Figure 11: Continued.

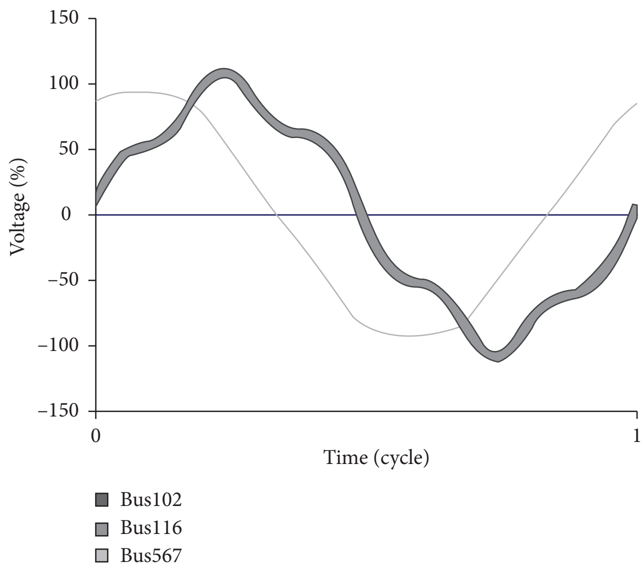

(e)

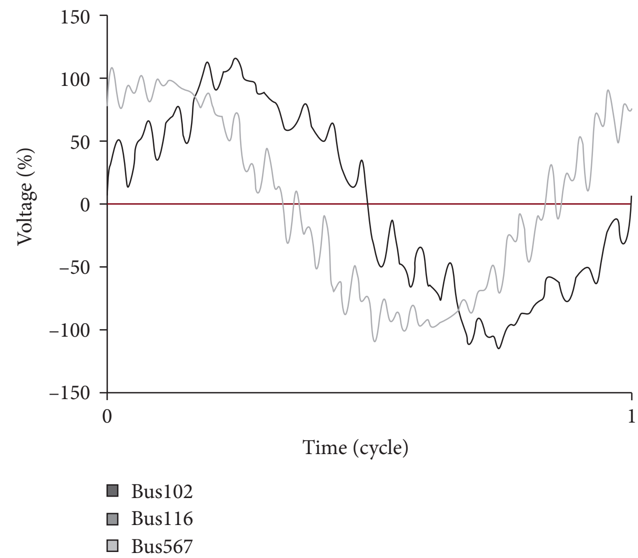

(f)

Figure 11: Spectrum view of harmonics order and harmonic waveform at different buses: (a, d) harmonic spectrum and waveform for the current situation, respectively; (b, e) harmonic spectrum and waveform for the centralized case, respectively; (c, f) harmonic spectrum and waveform for the decentralized case.

Table 5: Cost and system assumptions.

Variable	Quantity	Unit
Electricity selling price (both cases)	0.10	\$/kWh
Operation and maintenance (O & M; both cases)	25	\$/kW/year
Civil works (centralized PV system)	\$76,412.64	\$
Maintenance engineers (both cases)	1,000	\$/month
Inflation rate (both cases)	3%	—
Minimum attractive rate of return (both cases)	12%	—
Tax rate (both cases)	10%	—
Price of PV system (rooftop)	700	\$/kW
Price of PV system (land)	850	\$/kW
Plant power substation (centralized PV system)	\$45,847.58	\$
Yield factor of PV system	1750	kWh/kW/year
Roof rent	6	\$/m^2/year
Land	\$42,313.65	\$/dunam
Degradation	0.8	%/year
Salvage value	0	\$
Operational period	20	Year

can be seen in Figure 6. The symbols of the photovoltaic panel are the proposed rooftop PV systems.

On the other hand, the centralized system case is represented by a new 5 MW project, Figures 7 and 8 show the thermal contouring map of the centralized and decentralized cases, respectively.

The voltage profile of the network is indicated in Figure 9. In many buses, the voltage levels are under the IEEE power networks voltage standard (±5% p.u.). Although in the decentralized case, it is much better than other arguments, as it supports the voltage of buses and overloaded transformers.

The active power loss in the base case is reduced by 4.43% when the centralized case is used, whereas it is reduced by 13.43% when the decentralized case is used. Furthermore, the reactive power loss in the base case is reduced by 2.6% when the centralized case is used, whereas it is reduced by 14.49% when the decentralized case is used. Figure 10 represents the values of losses.

From Table 2, it is very clear that the centralized PV system reduced the loading of the point of common coupling and drew more reactive power. Such a case will make this point more underloaded and may increase the frequency level there that may negatively affect the frequency level of the network.

Based on Table 2, the installation of large PV system in a single location is not recommended, because of reverse power flow, significant losses of power, and overloading of

Table 6: Economic analysis of the centralized system.

EOY	O & M + engineers	Savings	Net savings	Depreciation	Total	Taxable income	Tax	ATCF	ATCF with inflation	Balance
0					($4,837,710)			($4,837,710)	($4,837,710)	($4,837,710)
1	($137,000)	$875,000.00	$738,000	($241,886)		$496,114	$49,611	$787,611	$764,671	($4,073,039)
2	($137,000)	$868,000.00	$731,000	($241,886)		$489,114	$48,911	$779,911	$735,141	($3,337,898)
3	($137,000)	$861,056.00	$724,056	($241,886)		$482,170	$48,217	$772,273	$706,739	($2,631,158)
4	($137,000)	$854,167.55	$717,168	($241,886)		$475,282	$47,528	$764,696	$679,422	($1,951,736)
5	($137,000)	$847,334.21	$710,334	($241,886)		$468,449	$46,845	$757,179	$653,149	($1,298,587)
6	($137,000)	$840,555.54	$703,556	($241,886)		$461,670	$46,167	$749,723	$627,881	($670,706)
7	($137,000)	$833,831.09	$696,831	($241,886)		$454,946	$45,495	$742,326	$603,579	($67,127)
8	($137,000)	$827,160.44	$690,160	($241,886)		$448,275	$44,827	$734,988	$580,206	$513,079
9	($137,000)	$820,543.16	$683,543	($241,886)		$441,658	$44,166	$727,709	$557,728	$1,070,807
10	($137,000)	$813,978.82	$676,979	($241,886)		$435,093	$43,509	$720,488	$536,111	$1,606,918
11	($137,000)	$807,466.99	$670,467	($241,886)		$428,581	$42,858	$713,325	$515,321	$2,122,239
12	($137,000)	$801,007.25	$664,007	($241,886)		$422,122	$42,212	$706,219	$495,328	$2,617,567
13	($137,000)	$794,599.19	$657,599	($241,886)		$415,714	$41,571	$699,171	$476,101	$3,093,669
14	($137,000)	$788,242.40	$651,242	($241,886)		$409,357	$40,936	$692,178	$457,611	$3,551,280
15	($137,000)	$781,936.46	$644,936	($241,886)		$403,051	$40,305	$685,242	$439,830	$3,991,110
16	($137,000)	$775,680.97	$638,681	($241,886)		$396,795	$39,680	$678,361	$422,732	$4,413,842
17	($137,000)	$769,475.52	$632,476	($241,886)		$390,590	$39,059	$671,535	$406,289	$4,820,132
18	($137,000)	$763,319.72	$626,320	($241,886)		$384,434	$38,443	$664,763	$390,478	$5,210,610
19	($137,000)	$757,213.16	$620,213	($241,886)		$378,328	$37,833	$658,046	$375,274	$5,585,884
20	($137,000)	$751,155.45	$614,155	($241,886)		$372,270	$37,227	$651,382	$360,655	$5,946,539

the network due to the low local demand at the suggested bus.

On the other hand, the suggested decentralized systems improve the voltage and reduce the losses. Table 3 illustrates the number of under-/overvoltage buses and overloaded transformers in the three cases (in the critical situation).

5.3. Results of Short-Circuit Analysis. The results of the three-phase short-circuit simulations performed for the grid in the current situation, centralized cases, and decentralized cases are presented in Table 4.

For the initial situation, the highest short-circuit current is 64.85 kA on the supply point. The implementation of the centralized case will lead to an increase of the short-circuit values within the analyzed network by 4.11%, while in the decentralized case, the increase in short-circuit current is 6.3%. However, the short-circuit security margin for the network will be at least 20% from the rated short-circuit current of the equipment after the implementation of the PV plant within the area. Therefore, there are no problems associated to short-circuit levels caused by the implementation of the PV plant.

5.4. Results of Power Quality Assessment. The impact of the proposed PV system on the harmonic content at the point of common coupling is investigated by harmonics load flow analysis. The harmonic voltages inside the PV system and at the point of common coupling are judged based on the IEC 61000-3-6 Standard by measuring the total harmonic distortions (THD). In practical considerations, the THD limit in MV and high-voltage networks is usually lowered to 5% and 2.5%, respectively, as required in the IEEE 519 Standard. In case the above limits are violating the IEEE standard, a harmonics violation case is reported in this study. The network currently faces a hard situation of harmonics, whereas at some points and cases, it reaches 17% at the fifth and the seventh components as THD. Based on that, IEEE 18 plus CT harmonic model is implemented for all grid components to describe approximately the harmonics situation in the grid.

The PV inverters are modeled as current injection sources. The considered spectrum is taken from typical manufacturer data, multiplied by a scaling factor to obtain the current THD of 3%, which is a usual value for such equipment. The simulation results are presented in Figure 11.

According to the results, many buses exceed the limits of the allowed harmonics in the grid. The main reason for that is the current situation of the harmonics in the grid due to the presence of nonlinear loads such as saws. It is extremely so high and needs mitigation. The centralized case does not contribute that much to this critical situation. However, it is found that the decentralized case may contribute negatively to the grid as the number of inverters increase as can be seen in Figures 11(c) and 11(f).

6. Brief Economic Analysis of the Proposed Systems

To illustrate how the economic analysis was carried out, the houses and transformers were given from the Tubas network on GIS. Then rooftops for the suggested capacities of PVDG were chosen based on $10\,m^2/kWp$.

The cost and system assumptions are presented in Table 5. Meanwhile, the economic analyses of both options are illustrated in Tables 6 and 7.

Capital cost includes the initial cost of installing a PV system. The operating cost includes the cost associated with maintaining and operating the PV system over its useful life. The analysis was carried out with consideration of taxes and depreciation.

Table 7: Economic analysis of the decentralized system.

EOY	O & M + engineers	Roof rent	Savings	Net savings	Depreciation	Total	Taxable income	Tax	ATCF	ATCF with inflation	Balance
0						($2,964,360)			($2,964,360)	($2,964,360)	($2,964,360)
1	($117,870)	($254,088)	$741,090.00	$369,132	($148,218)		$220,914	$22,091	$391,223	$379,829	($2,584,531)
2	($117,870)	($254,088)	$735,161.28	$363,203	($148,218)		$214,985	$21,499	$384,702	$362,618	($2,221,913)
3	($117,870)	($254,088)	$729,279.99	$357,322	($148,218)		$209,104	$20,910	$378,232	$346,136	($1,875,777)
4	($117,870)	($254,088)	$723,445.75	$351,488	($148,218)		$203,270	$20,327	$371,815	$330,353	($1,545,424)
5	($117,870)	($254,088)	$717,658.18	$345,700	($148,218)		$197,482	$19,748	$365,448	$315,239	($1,230,185)
6	($117,870)	($254,088)	$711,916.92	$339,959	($148,218)		$191,741	$19,174	$359,133	$300,768	($929,417)
7	($117,870)	($254,088)	$706,221.58	$334,264	($148,218)		$186,046	$18,605	$352,868	$286,914	($642,503)
8	($117,870)	($254,088)	$700,571.81	$328,614	($148,218)		$180,396	$18,040	$346,653	$273,651	($368,852)
9	($117,870)	($254,088)	$694,967.24	$323,009	($148,218)		$174,791	$17,479	$340,488	$260,956	($107,896)
10	($117,870)	($254,088)	$689,407.50	$317,449	($148,218)		$169,231	$16,923	$334,373	$248,805	$140,909
11	($117,870)	($254,088)	$683,892.24	$311,934	($148,218)		$163,716	$16,372	$328,306	$237,175	$378,084
12	($117,870)	($254,088)	$678,421.10	$306,463	($148,218)		$158,245	$15,825	$322,288	$226,046	$604,130
13	($117,870)	($254,088)	$672,993.73	$301,036	($148,218)		$152,818	$15,282	$316,318	$215,397	$819,527
14	($117,870)	($254,088)	$667,609.78	$295,652	($148,218)		$147,434	$14,743	$310,395	$205,208	$1,024,735
15	($117,870)	($254,088)	$662,268.90	$290,311	($148,218)		$142,093	$14,209	$304,520	$195,460	$1,220,195
16	($117,870)	($254,088)	$656,970.75	$285,013	($148,218)		$136,795	$13,679	$298,692	$186,135	$1,406,330
17	($117,870)	($254,088)	$651,714.99	$279,757	($148,218)		$131,539	$13,154	$292,911	$177,216	$1,583,546
18	($117,870)	($254,088)	$646,501.27	$274,543	($148,218)		$126,325	$12,633	$287,176	$168,686	$1,752,231
19	($117,870)	($254,088)	$641,329.26	$269,371	($148,218)		$121,153	$12,115	$281,487	$160,528	$1,912,759
20	($117,870)	($254,088)	$636,198.62	$264,241	($148,218)		$116,023	$11,602	$275,843	$152,728	$2,065,487

Table 8: Results of economic assessment.

	Decentralized	Centralized
NPV	−$768,212.88	−$246,021.02
RoR	7%	11%
SPP	9.434	7.116

The capital cost of the system was calculated based on PV system costs in addition to costs of plant substation, civil works, and land costs. Meanwhile, in case of the installation of a decentralized PV system, the cost of PV system is assumed to be equal to PV capital cost only. The O & M and salary of maintenance engineers were also considered together. The savings indicated in Tables 6 and 7 are the amount of electricity generation from the system, which is sold to the Tubas network by considering the degradation rate for each year. The net savings are the savings minus O & M and the salary of the engineers. The depreciation was calculated based on the straight-line method, taking the initial cost minus the salvage value divided by the operational period, which is 20 years.

After that, taxable income was calculated as net savings minus depreciation to know how much taxes would be paid. After-tax cash flow is net savings minus taxes. For SPP, a balance for the cash flow considering the inflation rate was carried out to have accurate results. The NPV, RoR, and SPP are presented in Table 8.

In general, although the decentralized system exceeds the centralized system technically, the centralized system seems to be slightly more profitable than the decentralized system. However, the decentralized system is still acceptable considering the technical flows that the centralized system may cause.

7. Conclusion

In this paper, a grid impact assessment of a photovoltaic-based distributed generation unit is proposed for a medium voltage distribution network. The paper also proposes a comparison based on grid assessment results between centralized and decentralized photovoltaic-based distributed generation. The comparison considered the power flow analysis, short-circuit analysis, and harmonic contribution of both cases. In addition to that financial analysis was also done for both cases for better comparison. The adapted case in this research was a real case that implies the real power flow performance of a medium voltage distribution network. Results showed that the decentralized PV distributed generation systems exceeds the centralized PV systems considering power flow analysis. Meanwhile, both cases were almost equal considering short-circuit contribution. Finally, the centralized PV system contributed fewer in terms of harmonic to the grid as compared to decentralized PV systems. On the other hand, the decentralized PV systems option was less profitable as compared to the centralized system. However, considering the technical implications of the centralized system, the decentralized PV systems were recommended.

Data Availability

Data are available upon request to the corresponding author.

Disclosure

The article is based on a BSc final year research.

Conflicts of Interest

The authors declare that they have no conflicts of interest.

References

[1] M. AlMuhaini, "Impact of distributed generation integration on the reliability of power distribution systems," in *Distributed Generation Systems*, G. B. Gharehpetian and S. M. Mousavi Agah, Eds., Butterworth-Heinemann, Oxford, UK, pp. 453–508, 2017.

[2] K. Tamer and E. Wilfried, "PV systems in the electrical power system," in *Modeling of Photovoltaic Systems Using MATLAB®*, pp. 159–174, Wiley, Hoboken, NJ, USA, 2016.

[3] M. Thomson and D. G. Infield, "Impact of widespread photovoltaics generation on distribution systems," *IET Renewable Power Generation*, vol. 1, no. 1, pp. 33–40, 2007.

[4] M. Karimi, H. Mokhlis, K. Naidu, S. Uddin, and A. H. A. Bakar, "Photovoltaic penetration issues and impacts in distribution network—a review," *Renewable and Sustainable Energy Reviews*, vol. 53, pp. 594–605, 2016.

[5] B. P. Koirala, B. Sahan, and N. Henze, "Study on MPP mismatch losses in photovoltaic applications," in *Proceedings of the Fraunhofer IWES*, Hamburg, Germany, September 2014.

[6] S. Shivashankar, S. Mekhilef, H. Mokhlis, and M. Karimi, "Mitigating methods of power fluctuation of photovoltaic (PV) sources—a review," *Renewable and Sustainable Energy Reviews*, vol. 59, pp. 1170–1184, 2016.

[7] M. S. ElNozahy and M. M. A. Salama, "Technical impacts of grid-connected photovoltaic systems on electrical networks-a review," *Journal of Renewable and Sustainable Energy*, vol. 5, no. 3, Article ID 032702, 2013.

[8] D. Cheng, B. A. Mather, R. Seguin, J. Hambrick, and R. P. Broadwater, "Photovoltaic (PV) impact assessment for very high penetration levels," *IEEE Journal of Photovoltaics*, vol. 6, no. 1, pp. 295–300, 2016.

[9] I. Taczi, B. Hartmann, and I. Vokony, "Impact study of smart grid technologies on low voltage networks with high penetration of renewable generation," *International Journal of Renewable Energy Research-IJRER*, vol. 10, no. 2, 2020.

[10] A. Kharrazi, V. Sreeram, and Y. Mishra, "Assessment techniques of the impact of grid-tied rooftop photovoltaic generation on the power quality of low voltage distribution network—a review," *Renewable and Sustainable Energy Reviews*, vol. 120, Article ID 109643, 2020.

[11] N. B. G. Brinkel, M. K. Gerritsma, T. A. AlSkaif et al., "Impact of rapid PV fluctuations on power quality in the low-voltage grid and mitigation strategies using electric vehicles," *International Journal of Electrical Power & Energy Systems*, vol. 118, Article ID 105741, 2020.

[12] A. Abualkhair, "Electricity sector in the Palestinian territories: which priorities for development and peace?" *Energy Policy*, vol. 35, no. 4, pp. 2209–2230, 2007.

[13] A. Juaidi, F. G. Montoya, I. H. Ibrik, and F. Manzano-Agugliaro, "An overview of renewable energy potential in Palestine," *Renewable and Sustainable Energy Reviews*, vol. 65, pp. 943–960, 2016.

[14] M. S. Ismail, M. Moghavvemi, and T. M. I. Mahlia, "Analysis and evaluation of various aspects of solar radiation in the

Palestinian territories," *Energy Conversion and Management*, vol. 73, pp. 57–68, 2013.

[15] A.-K. Daud and M. S. Ismail, "Design of isolated hybrid systems minimizing costs and pollutant emissions," *Renewable Energy*, vol. 44, pp. 215–224, 2012.

[16] M. A. Omar and M. M. Mahmoud, "Grid connected PV-home systems in Palestine: a review on technical performance, effects and economic feasibility," *Renewable and Sustainable Energy Reviews*, vol. 82, pp. 2490–2497, 2018.

[17] E. Ajlouni and H. Alsamamra, "A review of solar energy prospects in Palestine," *American Journal of Modern Energy*, vol. 5, no. 3, pp. 49–62, 2019.

[18] Y. Fathi Nassar and S. Yassin Alsadi, "Assessment of solar energy potential in Gaza Strip-Palestine," *Sustainable Energy Technologies and Assessments*, vol. 31, pp. 318–328, 2019.

[19] Palestinian Investment Promotion Agency, Renewable Energy Sector VP Booklet, Palestinian Investment Promotion Agency, Ramallah, Palestine, Report, http://www.pipa.ps/files/file/Value%20Proposition/EN/PIPA-%20Renewable%20Energy%20Sector%20VP%20Booklet-%20English.pdf.

[20] O. A. Afolabi, W. H. Ali, P. Cofie, J. Fuller, P. Obiomon, and E. S. Kolawole, "Analysis of the load flow problem in power system planning studies," *Energy and Power Engineering*, vol. 07, no. 10, pp. 509–523, 2015.

[21] H. Saadat, *Power System Analysis*, Tata McGraw Hill Education Pvt. Ltd, New York, NY, USA, 2010.

[22] D. P. Kothari and I. J. Nagrath, *Modern Power System Analysis*, Tata McGraw Hill Education Pvt., New York, NY, USA, 3rd edition, 2007.

[23] S. A. Soman, S. A. Khaparde, and S. Pandit, "Short circuit analysis," in *Computational Methods for Large Sparse Power Systems Analysis: An Object Oriented Approach*, S. A. Soman, S. A. Khaparde, and S. Pandit, Eds., Springer, Boston, MA, USA, pp. 179–212, 2002.

[24] S. H. Al-Saiari, "Analysis of power systems under normal and fault conditions," 2012, https://www.semanticscholar.org/paper/Analysis-of-power-systems-under-normal-and-fault-Al-Saiari/160b8613325c3172c53ced3b9ed83a0193a6d044.

[25] J. C. Das, *Power System Analysis: Short-Circuit Load Flow and Harmonics*, CRC Press, Boca Raton, FL, USA, 2002.